ELSEVIER

Biochimica et Biophysica Acta 1562 (2002) 37–44

BIOCHIMICA ET BIOPHYSICA ACTA
BBA

www.bba-direct.com

Magainin 2 in phospholipid bilayers: peptide orientation and lipid chain ordering studied by X-ray diffraction

Christian Münster [a], Alexander Spaar [a], Burkhard Bechinger [b], Tim Salditt [a,*]

[a] *Experimentalphysik, Universität des Saarlandes, Postfach 15 11 50, 66041 Saarbrücken, Germany*
[b] *Institut Le Bel, Université Louis Pasteur, 4, rue Blaise Pascal, F-67000 Strasbourg, Germany*

Received 13 November 2001; received in revised form 10 January 2002; accepted 17 January 2002

Abstract

We present a structural study of biomimetic lipid bilayers interacting with the antimicrobial peptide magainin 2 amide, using grazing incidence X-ray diffraction and reciprocal space mapping (RSM) techniques. The short-range order of lipid chains in lecithin is found to be strongly reduced by the peptides. From the scattering intensity of the chain correlation peak, we can quantify the lateral length scale R over which the bilayer structure is affected by peptide binding. The non-local perturbation of the bilayer is discussed in the framework of bilayer elasticity theory. © 2002 Elsevier Science B.V. All rights reserved.

Keywords: X-ray diffraction; Antibiotic peptide; Lipid–peptide interaction

1. Introduction

Membrane-active peptides play an important role in the innate immune system of animals. A wide variety of peptides have been discovered, for example in insects, amphibians but also in humans [1,2]. One of the best characterized is the 23-residue peptide magainin 2 from the skin granular gland of the African clawed frog *Xenopus laevis* [3]. Its broad bacteriocidal, fungicidal and virucidal activities help to protect the host organism from infection. There is good evidence that these peptides develop their lytic activity by interacting with lipid bilayers [3,4]. Although the detailed mechanism remains a matter of discussion, studying the interaction of antimicrobial peptides with phospholipid membranes is an active field of research relevant both to biological and pharmaceutical sciences [4–6]. Valuable insight into the structural mechanism of antibiotic activity can be derived from simple model systems composed of only a few, well-defined molecular components such as phospholipid membranes consisting of only one synthetic lipid component and peptides at various concentrations.

In the case of magainin, several studies conducted earlier have led to the following picture: magainins interact directly with the microbial cell membrane rather than with specific membrane proteins [11–13], subsequently causing an increase in membrane permeability and leading to cell lysis. The mode of interaction is strongly dependent on physiochemical properties [7], not only of the peptide, but also of the target membrane. By NMR spectroscopy, magainins were shown to be randomly coiled in aqueous solution and to assume right-handed α-helical conformations in the presence of phospholipid bilayers or organic solvents (reviewed in Ref. [12]). Helical wheel analysis of the 23-residue sequence GIGKFLHSAKKFGKAFVGEIMNS-amide shows one side of the helix to be hydrophobic and positively charged (4–5 positive net charges per molecule at neutral pH) while the other is hydrophilic and cationic. Therefore, an in-plane binding state with the hydrophobic side groups indented into the lipid chain region seems plausible, see Fig. 1(b). The in-plane association of the peptide has indeed been observed by oriented NMR, CD, ATR-FTIR and fluorescence energy transfer spectroscopies [8–10,14].

Furthermore, Ludtke et al. [14] have found a transition from a parallel state of the helical axis at low and medium peptide concentrations, to a normal orientation interpreted as part of an oligomeric channel-forming process, see Fig. 1(a). The authors report a phase of highly correlated, hard-disk-like oligomeric channels in the charged binary lipid system DMPC/DMPG, as deduced from a sharp interference maximum observed by in-plane neutron scattering [15,16].

* Corresponding author. Tel.: +49-681-302-2216; fax: +49-681-302-2819.
E-mail address: salditt@mx.uni-saarland.de (T. Salditt).

PII: S0005-2736(02)00357-7

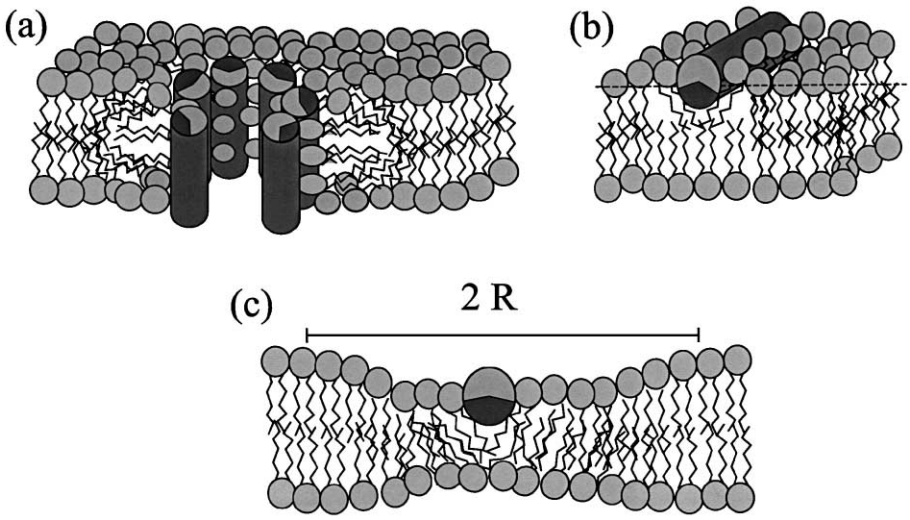

Fig. 1. Conformations of magainin 2 at the lipid bilayer, as proposed in the literature: (a) transmembrane orientation (insertion) and aggregation leading to the formation of oligomeric pores. The hydrophobic side groups are represented by the dark gray shade, the hydrophilic side groups by the lighter gray shade of the cylinder segments. (b) Adsorption state with the helical axis parallel to the bilayer. (c) The effect of the peptide on the acyl chain ordering within an interaction region of radius R.

Structural information on peptide–lipid systems at the molecular level is difficult to obtain. In the case of neutron and X-ray scattering, the amount of molecular information which can be derived is limited compared, e.g. to crystallographic studies, since the molecules lack long-range order in the fluid L_α state of the bilayer [17]. Nevertheless, subnanometer resolution of the peptide positions along the vertical z-axis can be achieved by diffraction from isotropic suspensions [18]. Contrarily, the in-plane structure of the bilayer can be studied in oriented stacks using synchrotron radiation or advanced neutron instruments [19–22]. To investigate the molecular arrangement in the plane of the bilayer, we have recently used the technique of grazing incidence diffraction (GID) to probe the acyl chain packing in the fluid L_α at various concentrations of the peptide magainin 2 [23]. The short-range order of the hydrocarbon tails in lecithin was found to be dramatically affected by the amphiphilic peptides. A clearer and more quantitative picture of this phenomenon arises in the present work, owing to a more complete data set, including two-dimensional reciprocal space mappings (RSM) along the vertical q_z and parallel $q_\parallel = \sqrt{q_x^2 + q_y^2}$ axis, see Fig. 2. Different aspects of the scattering geometry, in particular the refraction effects related to q_x- and q_y-scans, respectively, have been discussed in Ref. [24]. In contrast to one-dimensional line-scans, global features in reciprocal space can be identified more easily. Importantly, the intramolecular interference signal of the α-helices, e.g. the α-helical form factor can be probed in the RSM. The observed intensity distribution could be explained by a transition from a bound state parallel to the membrane to a transmembrane inserted state, in agreement with previous spectroscopic results [14]. Apart from the orientation of the helical axis, the diffraction experiment can give additional structural parameters, such as the helical pitch P, which may vary depending both on the bilayer properties and the peptide conformation.

In order to apply interface-sensitive scattering methods [25,26], a precise distinction between the momentum transfer parallel $q_\parallel$ and perpendicular q_z to the membranes is needed. A high degree of orientational alignment (with respect to the solid surface) is therefore required. In the present study of magainin 2 in neutral membranes of dimyristoylphosphatidylcholine (DMPC), the mosaicity of the samples was below the resolution limit (0.01°) [27,28]. Apart from structural studies, one can also study fluctuations on the mesoscopic scale in such systems. To this end, X-rays and neutrons offer the advantage to be compatible with in situ experiments at the relevant conditions of humidity, temperature and chemical potential. In particular, oriented bilayers can also be studied at full hydration while immersed in water [29].

2. Materials and methods

2.1. Peptide synthesis

Magainin 2 amide (*GIGKFLHSAKKFGKAFVGEIMNS*) was prepared by solid-phase peptide synthesis as described in Ref. [24]. The peptide was purified by reversed phase HPLC, and the high purity of the peptides was further analysed by matrix-assisted laser desorption mass spectrometry (MALDI-MS).

2.2. Lipids and sample preparation

1,2-dimyristoyl-sn-glycero-3-phosphatidylcholine (DMPC) was bought from Avanti (Birmingham, AL), and

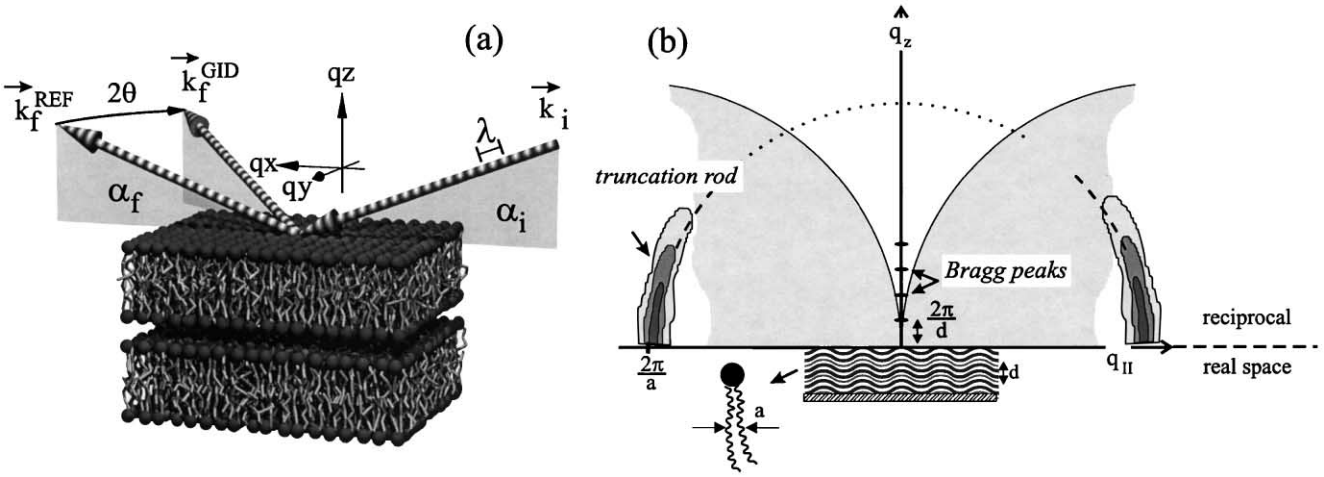

Fig. 2. (a) Sketch of the scattering geometry in (a) real and in (b) reciprocal space. (a) In grazing incidence diffraction (GID) the diffracted beam is measured out of the plane of incidence at an angle 2θ, while the angle of incidence α_i and exit α_f are kept close to the critical angle α_c. In the reciprocal space mappings (RSM), α_f and 2θ are varied over a wide range corresponding to wide-range mappings of $q_{\parallel}$ and q_z. In the RSM, the truncation-rod-like scattering of the acyl chain ordering is observed, and upon peptide partitioning additionally also the pitch peaks of the helical form factor. The light gray shaded area is not accessible by scattering in the plane of incidence [24].

was used without further purification. Multilamellar bilayers of DMPC containing the appropriate amount of magainin 2 at varied concentrations were prepared on cleaned silicon (111) wafers by spreading from organic solution, following essentially the procedure described by Seul and Sammon [30]. It is important to simultaneously meet the solvation requirements for a lipid/peptide mixture and the wettability on the silicon wafer. For sample deposition, the substrates were cleaned, rendered hydrophilic and positioned in an exactly horizontal plane. The wafers were cleaned by subsequent washing in methanol and trichloroethylene, and made hydrophilic by washing in a 5 molar solution of KOH in ethanol for about a minute. Between each step, the wafers were thoroughly rinsed with ultra pure water (specific resistivity ≥ 18 MΩ cm, Millipore, Bedford, MA).

The lipid and peptide components were co-dissolved in the desired ratio (molar ratio P/L) in trifluoroethanol (TFE) at concentrations of 20 mg/ml, depending on the total mass to be deposited. A drop of 1 ml was then carefully spread onto the well-leveled and cleaned substrates, yielding film thicknesses of about $D \simeq 10$ μm. The spread solution was allowed to dry only very slowly in an almost closed chamber, with excess solvent placed close to the substrate to increase the ambient solvent vapor pressure. The slow evaporation process extending over more than 12 h prevented film rupture and dewetting, yielding a very uniform dry film. Remaining traces of solvent in the sample were removed by exposing the samples to high vacuum over 24 h. The films were then rehydrated in a hydration chamber while tempering in successive temperature cycles around the main phase transition of the lipid to anneal lamellar defects. The orientational alignment of the multilamellar stack (lipid bilayers) with respect to the substrate (mosaicity) was typically better than 0.01°. A very low mosaicity is a prerequisite to applying interface-sensitive X-ray scattering techniques for structural studies of solid-supported bilayers.

2.3. Sample environment

During the X-ray experiments, the solid-supported multilamellar films were kept in a closed temperature-controlled chamber. The chamber consists of two concentric aluminum cylinders, with kapton windows. The inner cylinder was kept at constant $T = 45$ °C by a flow of oil, connected to a temperature-controlled reservoir (Julabo, Germany) with PID-control. The space between the two cylinders was evacuated to minimize heat conduction. The temperature was measured close to the sample holder by a *Pt*100 sensor, indicating a thermal stability of better than 0.02 K over several hours. At the bottom of the inner cylinder, a water reservoir was filled with salt-free Millipore water, such that the sample was effectively facing a vapor phase of nominally 100% relative humidity. Despite the nominally full hydration condition, DMPC bilayers were typically swollen up to a repeat distance of only $d \simeq 50$ Å in the fluid L_α-phase, i.e. were only partially hydrated. This limited swelling of solid-supported lipid films observation is well known as the so-called vapor-pressure paradoxon [31,32]. Note, however, that upon partitioning of cationic peptides, the lipids did swell up to around 68 Å at $P/L = 0.05$.

2.4. X-ray experiment

The samples were routinely characterized by X-ray reflectivity at a high resolution in-house rotating anode reflectometer with a dynamic range of up to eight orders after correction of the diffuse background. The GID experiments were carried out at the experimental stations D4

(bending magnet) and BW2 (wiggler beamline) of the synchrotron radiation source at HASYLAB/DESY using photon energies of 20 and 17 keV, respectively. At BW2, the focussing mirror was moved out of the beam to reach the required energy, selected by a *Si*(111) double monochromator, with the second crystal slightly tuned out of the Bragg condition to suppress higher harmonics. The angular resolution was controlled by the monochromator and motorized slits.

3. Results

The lateral structure of the membranes on molecular length scales could be probed by measurements taken in the grazing incidence diffraction (GID) mode, see illustrating sketch in Fig. 2(a). This interface-sensitive scattering method has evolved over the last two decades as a powerful tool in surface and sub-surface analysis of crystalline solids [33]. The X-ray optics and refraction effects are used to efficiently discriminate against bulk background signal and to gain depth resolution. Here, we apply the method to a highly oriented stack of lecithin membranes to study the effect of magainin 2 on the lateral ordering of acyl chains. Compared to diffraction studies of monolayers, highly aligned multilamellar membranes offer the advantage of much higher signals and furthermore allow for the observation of true bilayer–mimetic systems.

The scattering cross-section as probed in grazing incidence diffraction can be written in distorted-wave Born approximation as [33]

$$\frac{d\sigma}{d\Omega} \propto |T_i(\alpha_i)T_f(\alpha_f)|^2 \, S(q_\parallel, q_z), \tag{1}$$

where $T_{i/f}$ denote the Fresnel transmission functions, which lead to the characteristic Vinyard peaks when α_i or α_f equals the critical angle α_c. In contrast to these optical effects, the structural information is contained in the structure factor

$$S(q_\parallel, q_z) = \langle | \int d\mathbf{r} \; \rho(\mathbf{r}) e^{i\mathbf{qr}} |^2 \rangle, \tag{2}$$

where the vertical scattering depth along z can be tuned by α_i and α_f.

In aligned bilayers, the electron density $\rho(\mathbf{r})$ is isotropic in the $\boldsymbol{x}$,y-plane. The reciprocal space needed to describe the system is therefore essentially two-dimensional (2D) defined by the vertical q_z and lateral $q_\parallel$ axis, respectively. Particular Fourier components of $\rho(\mathbf{r})$ can be sampled depending on the area of q_z, $q_\parallel$ space which is probed. At small q-values, the lamellar structure leads to quasi-Bragg peaks as well as diffuse Bragg sheets. At $q_\parallel \simeq 1.39$ Å^{-1}, the well-known structure factor maximum reflecting the acyl chain ordering is observed, as sketched schematically in Fig. 2(b). Upon peptide partitioning, this ordering is found to be strongly affected, see Fig. 3.

Fig. 3 shows reciprocal space mappings from highly aligned multilamellar DMPC/magainin systems at increasing molar peptide/lipid ratios (P/L) in the range of $q_z \in \{0, 1.23$ Å$^{-1}\}$, $q_\parallel \in \{0.01, 3.06$ Å$^{-1}\}$. The angle of incidence was set close to the critical angle α_c to $\alpha_i = 0.12°$. Both the exit angle and the out of plane angle 2θ were varied. The mappings are displayed in linear gray scale for the respective P/L values and give an excellent overview over the intensity distribution in reciprocal space. We will not discuss here the nonspecular, diffuse scattering close to the specular axis at $q_\parallel \simeq 0$ (horizontal bottom lines in the figure). This contribution reflects the bilayer stacking and the bilayer fluctuations, in particular the bending modes [28]. Rather we concentrate on the following in the acyl chain peak, which is observed as a rod-like scattering signal at $q_\parallel = 1.39$ Å^{-1}, and which is found to decrease significantly in intensity with P/L. In addition, an enhanced scattering signal at around $q_z = 1.0$ Å^{-1} and $q_\parallel = 0.3$ Å^{-1}, is observed for $P/L = 0.01$ and more

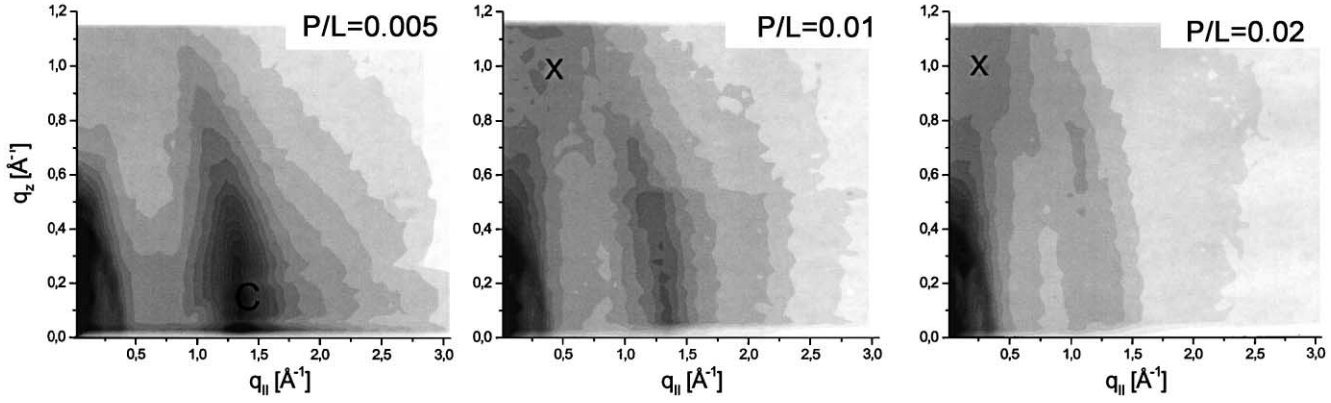

Fig. 3. Reciprocal space mappings of the magainin/DMPC system at P/L ratios of 0.005, 0.01, and 0.02, respectively, represented in linear gray shades. At a fixed incident angle of $\alpha_i = 0.2°$ the mapping was performed by varying α_f and 2θ at the BW2 wiggler beamline of Hasylab/Hamburg using 17 keV photons. At the low $q_\parallel$, q_z corner of the RSM, a tremendous amount of diffuse scattering intensity caused by correlated bilayer fluctuations is observed. In the present work, we discuss the wide angle region, where the acyl chain correlation peak (marked by 'c') is observed. Note also the much weaker signal (marked by 'x') observed in the $P/L = 0.01$ and $P/L = 0.02$ mappings, which is not observed at lower peptide concentrations or pure DMPC.

clearly at $P/L = 0.02$, but is absent in $P/L = 0$ (pure DMPC) and $P/L = 0.005$ samples. A possible explanation in terms of the form factor of the magainin helix is discussed further below.

The chain correlation peak (a so-called truncation rod in surface scattering) can be understood as the transform of the chain–chain positional correlation function, in an analogous way to the by-know classical scattering analysis of chain correlations in monolayer systems [34,35]. It decreases strongly with P/L, as the peptides partition into the bilayer. This effect can be observed in more detail in Fig. 4(a), which shows 1D slices in the reciprocal space at constant $q_z = 0.2$ Å^{-1} as a function of $q_\parallel$, for samples of increased peptide/lipid ratio (P/L). An understanding of the detailed nature of the peak may be gained by investigation of the Fourier transform of molecular dynamics (MD) data, showing that the peak at $q_\parallel = 1.39$ Å^{-1} corresponds to an average distance between the lipid acyl chains of $q_\parallel = 5.1$ Å. Such work is currently in progress. The peak line shape is Lorentzian, corresponding to an exponential decay of the chain–chain correlations with a decay length of 3.3 Å. The peak is strongly affected by the addition of magainin. Since the scattering volume is constant within a sample series, the measured scattering intensity can directly be interpreted in terms of acyl chain ordering. The tremendous loss of intensity can only be explained, if the chain ordering is reduced in an extended region around an adsorbed or inserted peptide. At small P/L, the peptides are assumed to adsorb with the helical axis parallel to the membrane in the headgroup region, intercalating between the lipids. This intercalation of hydrophobic side groups may result in a local strain field in the chains region, and possibly also in deviations from the equilibrium bilayer thickness δ [36,37]. Similar perturbations of the bilayer thickness have been postulated to result from the hydrophobic mismatch between a transmembrane protein and the bilayer. The perturbation caused by peptide partitioning may be relaxed only over a finite-range R parallel to the bilayer, as predicted by recent theories [38,39,41]. In order to evaluate the intensity decay quantitatively, we have to take into account the fact that apart from a decreasing peak at $q_\parallel = 1.395$ Å^{-1} (pure DMPC), there is a shoulder appearing at the lower $q_\parallel$ side of the peak, observed for samples of $P/L = 0.0005$ and $P/L = 0.001$, which develops into a second peak at $q_\parallel = 1.11$ Å^{-1} for $P/L = 0.02$ and $P/L = 0.1$. We discuss this side peak further below. Here, we simply take it into account by fitting a double-peak line shape (solid line). After sorting out the respective contributions and correcting for background, the intensities of the 1.39^{-1}-peak (scaled to pure DMPC) varies as 1, 0.48, 0.32, and 0.19 for $P/L = 0$, 0.005, 0.01, and 0.02, respectively.

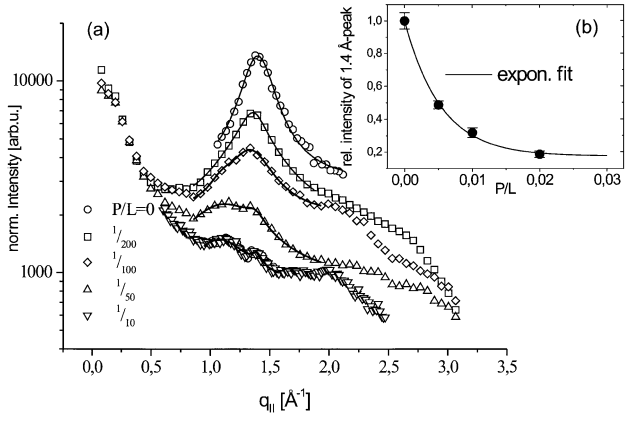

Fig. 4. Several line-scans taken at constant $q_z = 0.15$ Å^{-2} corresponding to cuts through the acyl chain peak are shown for increasing P/L. The curves are scaled according to the true intensity ratios, exhibiting a strong intensity decay with P/L. Note, that with increasing P/L ratio an additional peak at $q_\parallel = 1.11$ Å^{-1} occurs, see text for explanation. In the insert, the integrated intensity of the 1.4 Å^{-1} chain correlation peak is shown (normalized to pure DMPC), along with a fit to a single exponential decay.

The peak intensities of the 1.39 Å^{-1}-peak are plotted in Fig. 4(b), showing an exponential decay with P/L. This can be understood from a simple model, where peptides are randomly distributed in the plane of the membrane, according to a 2D Poisson-distribution point field. Assuming that each peptide in the plane affects a disk-shaped area of the bilayer with radius R, the fraction of the bilayer area which is not affected, i.e. the lipids which are further away from any of the randomly distributed peptides than R, varies like $e^{-c\pi R^2}$ [42], where c is the peptide concentration. We now assume that the scattering intensity can be written as the sum of two terms: (a) a constant residual intensity, I_{res}, describing the system if all chains are affected by the peptides, and (b) a second term which varies with the unaffected area of the bilayer. As a function of the variable P/L we then get

$$I(P/L) = I_{\mathrm{res}} + \Delta I \exp[-(P/L)\pi R^2/A_{\mathrm{L}}], \quad (3)$$

where ΔI is the difference in scattering intensity between the pure lipid chains and the scattering power of the lipids in the vicinity of the peptide, and A_{L} is the area per lipid headgroup. A least-square fit to this simple model equation is shown in Fig. 4(b), yielding a radius $R \simeq 62$ Å for $A_{\mathrm{L}} = 64^2$ Å, and a residual scattering intensity of 17%. In other words, peptide adsorption reduces the chain order in an area of about 12,000 Å^2 by more than 80%. This result convincingly underlines the cooperativity of the bilayer response to a local perturbation. Nevertheless, the weaknesses of the model becomes immediately apparent: (i) the statistical distribution of the peptides cannot be expected to be Poissonian if the peptides interact with each other, (ii) the model does not take into account oligomeric association, and (iii) the scattering power should change continuously with the distance from the peptide as the strain of the peptide is dissipated. Presently, however, the limited data set in Fig. 4 is well described by the simple model, which may be regarded as a zero order approach, which is sufficient until better data over wider range of P/L becomes available.

The result for R should be discussed in the framework of bilayer elasticity theory, which predicts that the bilayer perturbation due to an inserted peptide or protein relaxes over a length scale, which scales as [38,41]

$$\Lambda = (\delta\kappa/(4K_s))^{1/4}, \quad (4)$$

where δ is the equilibrium bilayer thickness, κ the bending rigidity and K_s the lipid layer stretching modulus (isothermal thickness compressibility modulus). For realistic values of $\kappa \simeq 25\ k_BT$ and $K \simeq 0.03\ k_BT/\text{Å}^3$, Λ is on the order of 10 Å. However, as pointed out by Huang [40], the thickness deformation profile may contain an inflection point, and as a result, a local deformation may propagate over several Λ. Furthermore, the lipid tilt degree of freedom, which has not been considered in the derivation of the above equation, is also expected to change the relaxation length [39]. The value of $R \simeq 60$ Å found in the present system is sufficiently close to the predictions and can help to validate the theoretic assumptions.

Having discussed the effect of the peptide-mediated decrease in the chain–chain correlation peak, which can be regarded as an indirect contribution of the peptides in the scattering pattern (RSM), let us now address the possibility of any direct contributions to the RSMs stemming from scattering from the peptides themselves. To this end, we have to discuss the form factor of the adsorbed or inserted peptides, which may be observable as an intra-molecular interference effect in oriented systems as a result of a very low background. If the peptides are uncorrelated in position, this scattering signal corresponds to a form factor $F(\mathbf{q})$ of the molecules, which are dissolved in the multilamellar bilayers without long-range positional order. However, the orientation of the molecules with respect to the bilayer may be expected to be ordered. Without any regular folding motive, it is difficult if not impossible to observe $F(\mathbf{q})$. Contrarily, secondary structural elements like β-sheet or α-helical folding, can be more easily detected.

A first qualitative understanding of the form factor contribution to the RSM can be gained by calculating the form factor $F(\mathbf{q})$ of the α-helix, for an idealized helix with each residue approximated by a point scatterer on the helix backbone, characterized by a pitch of $P = 5.4$ Å and a number of 3.6 scatterers per pitch. Rather than using the classical analytical expressions of Bessel functions [43], we have evaluated the form factor numerically over a 2D area in reciprocal space, after orientationally averaging the rotation angle ϕ of the molecule around its helical axis, see Fig. 5. The ϕ-averaging follows from the in-plane isotropy of the bilayer and the fact that the helix is expected to be oriented vertically at high P/L. Accordingly, the form factor is evaluated as

$$S(q_\parallel, q_z) = \frac{1}{2\pi}\int_0^{2\pi} d\phi \left| \sum_n f_n e^{-i(x_n q_\parallel \cos\phi + y_n q_\parallel \sin\phi + z_n q_z)} \right|^2, \quad (5)$$

with the z-axis normal to the plane of the membrane. f_n is the atomic form factor of scatterer n, which is set equal to one for all 23 residues alike. The diameter of the helix was set to 10 Å. The computed form factor corresponding to this 'artificial' α-helix is shown in Fig. 5(a), and has two well-known characteristic features. Firstly, the residue peak (R) at $q_z = 3.6\ (2\pi)/(P) = 4.2\ \text{Å}^{-1}$ located on the q_z-axis. Secondly, the off-axis intensity distribution of the pitch-peak (P) at $q_z = (2\pi)/(\text{pitch}) = 1.16\ \text{Å}^{-1}$ and $q_\parallel = \pm 0.73\ \text{Å}^{-1}$.

Since magainin 2 is known to be bent and the arrangement of the amino groups is asymmetric, an additional bending of the whole molecule along the helical axis can be easily introduced, as well as a more realistic arrangement of the point scatterers representing the amino side groups. The latter correction would essentially lead to a displacement of the point scatterers away from the helix to account for a center of mass shifted away from the backbone. Applying both corrections (in real space coordinates) leads

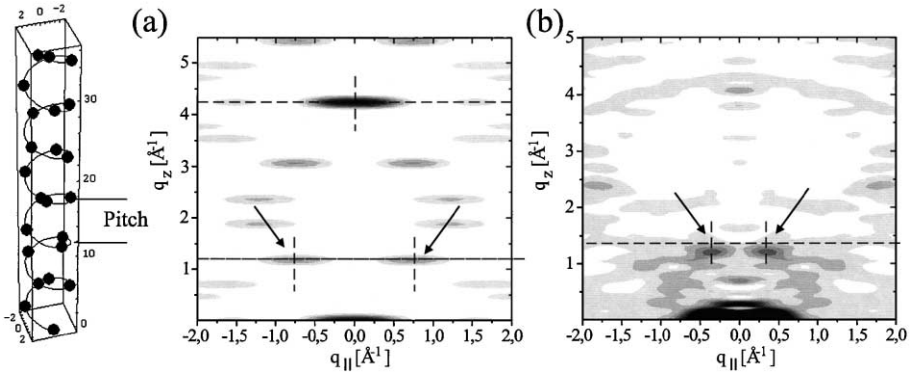

Fig. 5. (a) A simple model of the alpha helix: numerical form factor of 23 distinct scatterers arranged on a helix with diameter 10 Å pitch, $P = 5.4$ Å and 3.6 scatterers per pitch, shown in linear gray shade. The typical 'pitch peak' with the symmetrical the *eye-like* maxima at $q_z = 1.16\ \text{Å}^{-1}$ is observed (see arrows), as well as the 'residue' peak, $4.2\ \text{Å}^{-1}$. (b) Numerical form factor of magainin 2 calculated from the Brookhaven protein data base coordinates www.pdb.de). The residue peak of the ideal model (point scatterers on helix) is washed out, while the pitch peak is still clearly observed, but shifted towards the q_z-axis ($q_\parallel \simeq 0.35\ \text{Å}^{-1}$). Note that the strong scattering at the origin (primary beam position) is a finite-size artifact of the form factor.

to a decreasing $q_{\parallel}$-component of the pitch-peak in reciprocal space [44].

As an alternative to these 'toy' models, the solution–NMR structure coordinates [45] from the Brookhaven protein data bank www.rcsb.org/pdb) can be taken to compute the ϕ-averaged form factor, as shown in Fig. 5(b), displaying significant differences with respect to Fig. 5(a). In particular, the residue-peak at 4.2 Å^{-1} has vanished. Likewise, no residue-peak was found experimentally (scans not shown here). The off-axis pitch-peak is observed at 1.208 Å^{-1} and $q_{\parallel} = \pm 0.35$ Å^{-1}. With the simulation at hand, the questions arises whether the weak scattering features in Fig. 3 (marked by x) may be attributed to a broad tail of the pitch peak.

Two insufficiencies of the experimental data (Fig. 3) become obvious: (i) the interesting region for the helix peak is at the boundary of the RSM and (ii) the signal-to-background ratio is too weak. To overcome these problems, an additional RSM on a sample with high peptide concentration $P/L = 0.1$ was run over a wider range in q_z. The result is shown in Fig. 6. Note that the kapton window of the sample chamber (geometrical L-form) leads to shadowing in the upper right corner of the RSM. The weak intensity observed in the previous RSM (marked by 'x' in Fig. 3) now appears to be at the tail of a broad and more pronounced maximum located around $q_z = 1.4$ Å^{-1} and $q_{\parallel} = 0.4$ Å^{-1}. We tentatively attribute this maximum to a transmembrane helical peak with a pitch of $P = 4.5 \pm 0.2$, despite the fact that this value seems to be quite small even for transmembrane helices, where smaller pitch values are however not unusual [46–48]. In this case, a significant fraction of the peptides must be inserted at high P/L, which is in good agreement with spectroscopic results obtained from circular dichroism (CD) measurements [14]. Note, however, that the shoulder in the chain-correlation peak shown in Fig. 4(a), could also be attributed to a pitch-peak for an in-plane helix. Even though comparatively weak, a corresponding signal at $q_z = 0.4$ Å^{-1} and $q_{\parallel} = 1.4$ Å^{-1} is also observed in Fig. 6. Therefore, a co-existence of parallel and inserted peptides at high P/L, seems likely. Presently, the data is not sufficient to quantify the respective fractions. Apart from further investigations by X-ray scattering, complementary methods like CD spectroscopy on oriented bilayers are needed to shed more light on this point.

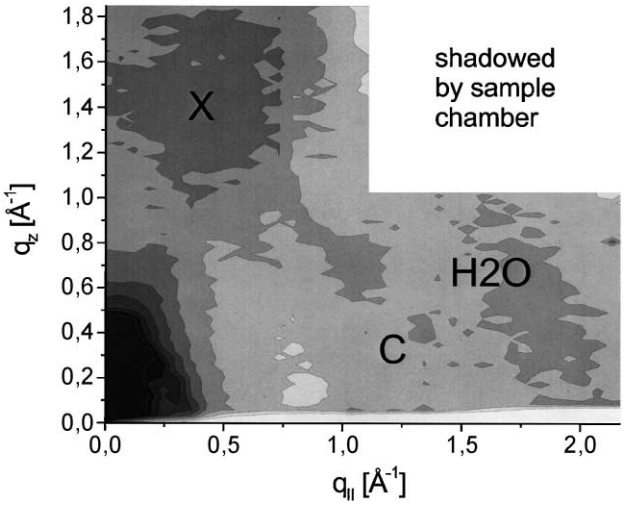

Fig. 6. Reciprocal space mapping at high peptide concentration $P/L = 0.1$ in linear gray shades. The chain–chain correlation peak (located around C) has tremendously decreased, and is now smaller than the water peak (H_2O) at around $q \simeq 2.0$ Å^{-1}. The water peak is more pronounced than at small P/L, since the bilayers swell due to the cationic peptide charges. Note that a pronounced maximum (X) appears around $q_z = 1.4$ Å^{-1} and $q_{\parallel} = 0.4$ Å^{-1}, which can be attributed a transmembrane helical pitch peak.

4. Summary

We have shown that RSM can be used to record and display the X-ray scattering signal of oriented bilayers. In particular, RSM can help to identify and distinguish individual scattering contributions. A strong effect on the lipid chain correlation peak was observed upon partitioning of magainin 2 amide in DMPC, asymptotically leading to a reduction in the integrated peak intensity of about 80% (Fig. 4(b)). From the intensity decay, a length scale $R \simeq 62$ Å (radius) could be deduced, over which the bilayer deformation, and correspondingly the acyl chain disorder, relaxes to its equilibrium configuration. A significant non-local effect of magainin 2 amide on the acyl chain ordering has thus been observed. The value of R can be understood in the framework of current bilayer elasticity models. Changes of R with the elastic and geometric properties of the bilayer remain to be investigated for different anionic and neutral lipids and put into perspective of the antibiotic function of magainin 2.

An enhanced scattering signal has been found in the RSM, close to the expected position of the (helix) pitch peak of the magainin form factor, presenting evidence for a transmembrane orientation at high P/L (Fig. 6). At the same time, a shoulder observed in the acyl chain correlation peak may be tentatively attributed to a population of peptides, which is adsorbed parallel to the bilayer (predominantly at small P/L according to the literature [14]. While an inserted state of the peptide must necessarily be accompanied by oligomeric pore formation, we have no experimental evidence for pore formation in our data. In particular, we did not find evidence for lateral correlations between channels or pores in the bilayer, as reported in Ref. [16].

Reciprocal space mappings of oriented bilayer systems may be used in the future to determine the orientation of membrane-bound peptides relative to the membrane surface. To predict and to model the scattering distributions, full atomic coordinates rather than an idealized helix model have to be used. The position of the pitch peak, for example, has been shown to differ in the two cases. In a future study, we plan to measure the helical pitch, P, of transmembrane

peptides as a function of hydrophobic chain length in model membranes. To this end, it is essential to achieve lower background levels than at present.

Acknowledgements

We thank Michael Vogel for help with the synchrotron measurements, and Susanne Schinzel for help with the peptide synthesis, HASYLAB/DESY for providing sufficient beamtime at the D4 and BW2 experimental stations. Financial aid by the Deutsche Forschungsgemeinschaft (DFG) through grants SA 772/3 and SA-772/4 is gratefully acknowledged.

References

[1] C.L. Bevins, M. Zasloff, Annu. Rev. Biochem. 59 (1990) 395–441.
[2] H.G. Boman, Cell 65 (1991) 205–207.
[3] B. Bechinger, Biochim. Biophys. Acta 1462 (1999) 157.
[4] Y. Shai, Biochim. Biophys. Acta 1462 (1999) 55.
[5] R.M. Epand, H.J. Vogel, Biochim. Biophys. Acta 1462 (1999) 11.
[6] K. Matsuzaki, Magainins as paradigm for the mode of action of pore forming polypeptides, Biochim. Biophys. Acta 1376 (1998) 391, and references therein.
[7] T. Wieprecht, PhD Dissertation, Math-Naturwiss. Fakultät I, Humboldt Universität Berlin (1997).
[8] B. Bechinger, M. Zasloff, S.J. Opella, Protein Sci. 2 (1993) 2077–2084.
[9] B. Bechinger, J.-M. Ruysschaert, E. Goormaghtigh, Biophys. J. 76 (1999) 552–563.
[10] K. Matsuzaki, O. Murase, H. Tokuda, S. Funakoshi, N. Fujii, K. Miyajima, Biochemistry 33 (1994) 3342–3349.
[11] M. Zasloff, Magainins, a class of antimicrobial peptides from *Xenopus* skin: isolation, characterization of two active forms, and partial cDNA sequence of a precursor, Proc. Natl. Acad. Sci. U.S.A. 84 (1987) 5449.
[12] B. Bechinger, Structure and functions of channel-forming polypeptides: magainins, cecropins, melittin and alamethicin, J. Membr. Biol. 156 (1997) 197–211.
[13] D. Wade, A. Boman, B. Wahlin, C.M. Drain, D. Andreu, H.G. Boman, R.B. Merrifield, All-D amino acid-containing channel-forming antibiotic peptides, Proc. Natl. Acad. Sci. U.S.A. 87 (1990) 4761–4765.
[14] S.J. Ludtke, K. He, Y. Wu, H.W. Huang, Cooperative membrane insertation of magainin correlated with its cytolytic activity, Biochim. Biophys. Acta 1190 (1994) 181–184.
[15] S.J. Ludtke, K. He, H.W. Huang, Membrane thinning caused by magainin 2, Biochemistry 34 (1995) 16764.
[16] S.J. Ludtke, K. He, W.T. Heller, T.A. Harroun, et al., Membrane pores induced by magainin, Biochemistry 35 (1996) 13723.
[17] J.F. Nagle, S. Tristram-Nagle, Structure of lipid bilayers, Biochim. Biophys. Acta 1469 (2000) 159–195.
[18] S.H. White, K. Hristova, Peptides in lipid bilayers: determination of location by absolute-scale X-ray refinement, in: J. Katsaras, T. Gutberlet (Eds.), Lipid Bilayers: Structure and Interactions, Springer, Berlin, 2000.
[19] G. Smith, E.B. Sirota, C.R. Safinya, N.A. Clark, Phys. Rev. Lett. 60 (1988) 813.
[20] J. Katsaras, X-ray diffraction studies of oriented lipid bilayers, Biochem. Cell Biol. (1995) 209–218.
[21] G. Fragneto, T. Charitat, F. Graner, K. Mecke, L. Perino-Gallice, E. Bellet-Amalrice, A fluid floating bilayer, Europhys. Lett. 53 (2001) 100–106.
[22] C. Gliss, H. Clausen-Schaumann, R. Günther, S. Odenbach, O. Randl, T.M. Bayerl, Direct detection of domains in bilayers by grazing incidence diffraction of neutrons and atomic force microscopy, Biophys. J. 74 (1998) 2443–2450.
[23] C. Münster, J. Lu, B. Bechinger, T. Salditt, Grazing incidence X-ray diffraction of highly aligned phospholipid membranes containing antimicrobial peptides magainin 2, Eur. Biophys. J. Biophys. Lett. 28 (2000) 683–688.
[24] C. Münster, T. Salditt, M. Vogel, J. Peisl, Nonspecular neutron scattering from highly aligned membranes, Europhys. Lett. 46 (1999) 486.
[25] J. Daillant, A. Gibaud (Eds.), X-ray and neutron reflectivity: principles and applications, Lecture Notes in Physics, vol. 58, Springer, Berlin, 1999.
[26] M. Tolan, X-ray scattering from soft-matter thin films, Springer Tracts Mod. Phys. (1999) 148.
[27] T. Salditt, Structure and fluctuations of highly oriented phospholipid membranes, Curr. Opin. Colloid Interface Sci. 5 (2000) 19–26.
[28] T. Salditt, Y. Lu, C. Münster, M. Vogel, W. Fenzl, A. Souvorov, Specular and diffuse scattering from highly aligned phospholipid membranes, Phys. Rev. E 60 (1999) 7285.
[29] M. Vogel, C. Münster, W. Fenzl, T. Salditt, Thermal unbinding of highly oriented phospholipid membranes, Phys. Rev. Lett. 84 (2000) 390–393.
[30] M. Seul, M.J. Sammon, Preparation of surfractant multilayer films on solid substrates by deposition from organic solution, Thin Solid Films 185 (1990) 287.
[31] R. Podgornik, V.A. Parsegian, On a possible microscopic mechanism underlying the vapor pressure paradox, Biophys. J. 75 (1997) 942–952.
[32] J.F. Nagle, J. Katsaras, Absence of a vestigial vapor pressure paradoxon, Phys. Rev. E 61 (1999) 7018–7024.
[33] H. Dosch, Critical phenomena at surfaces and interfaces, Springer Tracts Mod. Phys. (1992) 126.
[34] C.A. Helm, H. Möhwald, K. Kjaer, J. Als-Nielsen, Phospholipid monolayer density distribution perpendicular to the water surface. A synchrotron X-ray reflection study, Europhys. Lett. 4 (1987) 697–703.
[35] J. Als-Nielsen, H. Möhwald, in: S. Ebashi, E. Rubinstein, K. Koch (Eds.), Handbook of Synchrotron Radiation, vol. 4, North-Holland, Amsterdam, 1992, 3 pp.
[36] O.K. Härzer, B. Bechinger, Biochemistry 39 (2000) 13106.
[37] J.A. Killian, Biophys. Biochim. Acta 1376 (1999) 401–416.
[38] H.W. Huang, Elasticity of lipid bilayer interacting with amphiphilic helical peptides, J. Phys. II 5 (1995) 1427.
[39] S. May, Inclusion induced bilayer deformations: the lipid tilt degree of freedom, Eur. Biophys. J. 29 (2000) 17–28.
[40] H.W. Huang, Biophys. J. 50 (1986) 1061–1070.
[41] S. May, Theories on structural perturbations of lipid bilayers, Curr. Opin. Colloid Interface Sci. 5 (2000) 244–249.
[42] K.R. Mecke, Additivity, convexity, and beyond: applications of Minkowski functionals in statistical physics, in: Lecture Notes in Physics, vol. 554, Springer, Berlin, 2000.
[43] C.R. Cantor, P.R. Schimmel, Biophysical Chemistry, Freeman, New York, 1980.
[44] C. Münster, PhD Dissertation, Sektion Physik, Ludwig-Maximilians-Universität München (2000).
[45] J. Gesell, M. Zasloff, S.J. Opella, J. Biomol. NMR 9 (1997) 127, structure model No. 7.
[46] R. Henderson, J.M. Baldwin, T.A. Ceska, F. Zemlin, E. Beckmann, K.H. Downing, J. Mol. Biol. 213 (1990) 899.
[47] J. Katsaras, R.S. Prosser, R.H. Stinson, J.H. Davis, Biophys. J. 61 (1992) 827–830.
[48] J. Müller, C. Münster, T. Salditt, Biophys. J. 78 (2000) 3208–3217.